A general methodology for quantum modeling of free-energy profile of reactions in solution: An application to the Menshutkin NH_3+CH_3Cl reaction in water

Thanh N. Truong,[a] Thanh-Thai T. Truong, and Eugene V. Stefanovich
Department of Chemistry and Henry Eyring Center for Theoretical Chemistry, University of Utah, Salt Lake City, Utah 84112

(Received 4 March 1997; accepted 6 May 1997)

We present a general methodology for calculating free-energy profile of reaction in solution using quantum mechanical methods coupled with the dielectric continuum solvation approach. Particularly, the generalized conductorlike screening model (GCOSMO) was employed in this study, though any continuum model with existing free-energy derivatives could also be used. Free-energy profile is defined as the steepest descent path from the transition state to the reactant and product channels on the liquid-phase free-energy surface. Application of this methodology to calculate the free-energy profile of the Menshutkin NH_3+CH_3Cl reaction in water is discussed. The efficiency of the GCOSMO method allows characterization of stationary points and determination of reaction paths to be carried out at less than 20% additional computational cost compared to gas-phase calculations. Excellent agreement between the present results and previous Monte Carlo simulations using a combined quantum mechanical/molecular mechanics (QM/MM) potential confirms the accuracy and usefulness of the GCOSMO model. © *1997 American Institute of Physics.* [S0021-9606(97)52130-1]

I. INTRODUCTION

For the past half century, quantum chemistry has made significant progress in prediction properties of gas-phase processes. Theoretical efforts recently have been turning toward solution chemistry. Despite some progress has been made in developing predictive models for equilibrium and spectroscopic properties of molecules in solution, quantum modeling of free-energy profile in solution still remains a challenge.[1–3] Free-energy profiles are important for elucidating mechanisms of reactions in solution and addressing their dynamics. The challenge arises from the requirements that adequate theoretical models must have accurate description of both the bond-forming and -breaking processes and the solvent–solute interactions.

First, proper description of the bond-forming and -breaking processes requires an accurate correlated level of *ab initio* quantum mechanical theory. At the present time, it is computationally unfeasible to perform full *ab initio* quantum simulations for reactions in solution due to the large number of solvent molecules required. Although rapid progress is being made for quantum (electronic degrees of freedom only) simulations of equilibrium properties of condensed-phase systems with the use of Car–Parrinello approach,[4–6] in most theoretical studies so far, approximations were made to reduce the computational demand for calculating the solvent–solute interactions. These studies treat the solvent either explicitly or implicitly.

A. Explicit treatments of solvent–solute interaction

Within this approach, there are two general methodologies. The supermolecule model[7,8] treats a small number of first-solvation-shell solvent molecules explicitly at the same quantum mechanical level as the solute. This model offers a straightforward and accurate way to account for the localized portion of the solvent–solute interaction. However, it cannot include the long-range electrostatic interactions with the bulk solvent. Another common methodology is to construct an approximate solvent–solute interaction potential either using classical molecular mechanics force fields,[9] empirical valence bond method,[10] combined quantum mechanical/molecular mechanics (QM/MM) method,[11–14] or recent effective fragment method.[15] Then, for calculating reaction profiles in solution, one performs classical free-energy simulations to evaluate the potential of mean force along a selected reaction coordinate.

The advantage of approaches with explicit solvent is that they provide detailed solvation structure enabling one to elucidate specific roles of solvent in reaction mechanisms. The main difficulty of these models is the definition of the reaction coordinate. Due to the large number of solvent degrees of freedom there is no unique way to define a reaction coordinate. As a result, this approach relies on the gas-phase or a simple user-defined reaction coordinate. As a result, participation of solvent motions in the reaction coordinate is ignored. Such practice works reasonably well for many simple reactions. For complex reactions where competing reaction paths exist and solvent effects change the topology of the free-energy surface, one can in principle, examine all possible free-energy paths but this would be too costly. There are numerous examples of such complex cases. For instance, solvent effects change the prefered conformation of the transition state and the diastereofacial selectivity of the Diels–Alder reaction between cyclopentadiene and (-)-menthylacrylate.[16–18] Solvent can also change the reaction mecha-

[a]Author to whom correspondence should be addressed.

nism as seen in the ketene-imine cycloaddition in which the two-step mechanism is prefered in solution while the concerted mechanism was predicted for the gas phase.[19] Another example is a significant shift of the transition state toward the reactant channel in the Menshutkin NH_3+CH_3Cl reaction in aqueous solution.[20]

In general, the combined QM/MM approach in conjunction with molecular dynamics or Monte Carlo free-energy simulations would be the best way to provide accurate and detailed picture of reactions in solution. However, determination of the potential of mean force requires a large number of free-energy simulations, typically around 30–60 runs. This is quite time consuming and computationally expensive. Such an approach is useful to gain detailed fundamental knowledge for selected well-known reactions. It is, however, not practical for gaining first insight into the roles of solvent for assisting synthetic design of new materials. Here one needs a *cost effective* theoretical tool to provide reasonably accurate predictions to guide experiments.

B. Implicit treatments of solvent–solute interactions

Among several methodologies for implicit treatment of the solvent, the dielectric continuum approach[21–23] offers the simplest and yet reasonably accurate methodology. In the dielectric continuum approach, the solvated system is modeled as the solute (if necessary, with inclusion of several first-solvation-shell solvent molecules) inside a cavity surrounded by a dielectric continuum medium represented by the dielectric constant ϵ. Such model has several weaknesses. In particular, it does not provide any information on the solvent structure. In addition, the size and shape of the cavity have no rigorous definitions. However, there are also several important advantages. First, one can select a desired level of quantum mechanical theory from a wide range of *ab initio* molecular orbital (MO) and density functional theory (DFT) levels that is sufficiently accurate for modeling bond-breaking and forming processes. Second, the reaction coordinate is uniquely defined because solvent effects from the continuum medium are effectively included in the solute Hamiltonian and do not increase the dimensionality of the system. Third, availability of analytical free-energy derivatives greatly enhances the ability to explore the free-energy surface and to characterize stationary points. With appropriate choice of van der Waals radii for cavity construction, one can obtain reasonably accurate free energy of solvation for a wide range of solutes. Overall, for modeling reactions in solution the dielectric continuum approach provides the most cost effective methodology.

Most of previous dielectric continuum calculations of solvent effects on reaction mechanisms were based on simple (spherical or ellipsoidal) cavity models.[21,23] Although these self-consistent reaction field studies provide useful insight, their accuracy is often questionable due to the uncertainty in the cavity size and shape for variable geometry of the reacting system. For more realistic molecular-shape cavities, three models have shown some promise due to the availability of analytical free-energy derivatives. One is known as the polarizable continuum model (PCM).[23–27] Second is the reaction field factors formalism which is based on the Kirkwood multipole expansion model.[28,29] Third is the generalized conductorlike screening model (GCOSMO)[30–35] developed in our group that is based on an approximate scheme for scaling screening conductor surface charges originally proposed by Klamt and Schüürmann.[36] Implementation of the original COSMO approach to the density functional theory was also done by Andzelm *et al.*[37] However, to date a general methodology for following reaction paths on the solution-phase free-energy surface has not been developed.

In this study, we present a general methodology for calculating free-energy profiles in solution by following the minimum free energy path (MFEP) on the free-energy surface. Using the GCOSMO solvation model, we have carried out a systematic *ab initio* study of the Menshutkin $NH_3+CH_3Cl\leftrightarrow NH_3CH_3^++Cl^-$ reaction in aqueous solution. This is a type II S_N2 reaction which is different from the type I S_N2 charge transfer reactions, such as $Cl^-+CH_3Cl\rightarrow ClCH_3+Cl^-$, in several aspects. First, for the $Cl^-+CH_3Cl\rightarrow ClCH_3+Cl^-$ reaction solvent effects significantly decrease the reaction rate due to charge delocalization and decrease of the free energy of solvation at the transition state. In contrast, the rate of the Menshutkin reaction has been found to increase dramatically with increasing solvent polarity which favors charge separation and thus stabilizes the transition state. Second, the $Cl^-+CH_3Cl\rightarrow ClCH_3+Cl^-$ reaction is symmetric, thus one expects very little solvent effect on the transition state structure. In contrast, the Menshutkin reaction is an unsymmetric charge separation process with endothermicity of 110 kcal/mol in the gas phase but it is exothermic by about -34 ± 10 kcal/mol in aqueous solution due to the stabilization of the $H_3CNH_3^+$ and Cl^- ions by the solvent.[20] According to the Hammond postulate,[38] solvent effects would shift the transition state toward the reactant channel, thus solvent has a direct participation in the reaction coordinate. Such role of solvent challenges the validity of the static equilibrium solvation treatment which assumes solvent to be in equilibrium with the chemical system at each point along the gas-phase reaction coordinate. For this reason, the Menshutkin reaction provides a challenging test to any solvation theory attempting to model solvent effects on transition state structure and reaction profile.

Gao and Xia[20] recognized that for this reaction it is more appropriate to determine the MFEP in solution rather than to follow the gas-phase reaction coordinate. To do this, Gao and Xia have performed elaborated QM/MM simulations to map out a 2D free-energy surface. Transition state structure and the MFEP were then estimated from this 2D surface. Although these authors used rather approximate AM1 Hamiltonian for the solute, their QM/MM description of solvent–solute interactions was quite accurate and the AM1 barrier height happened to agree well with the free energy of activation for the gas-phase reaction. These results will be used below for assessing the accuracy of the GCOSMO solvation model. Another Menshutkin reaction, NH_3+CH_3Br, was studied by Sola *et al.*[39] using both the supermolecule and PCM approaches. The PCM results for the free energy of

activation appeared to be too low. This disagreement led Gao and Xia[20] to question the accuracy and applicability of the dielectric continuum approach for studying reactions of this type. Both PCM and QM/MM studies confirmed qualitatively the large solvent effect on the transition state. However, the transition state in solution has not been fully optimized and the full dimensional MFEP has not been calculated. In the present study, using the GCOSMO dielectric continuum methodology, we fully optimized the transition state of the Menshutkin $NH_3+CH_3Cl\leftrightarrow NH_3CH_3^+ + Cl^-$ reaction in aqueous solution and determined the minimum free-energy path in all degrees of freedom of the solute. Possible sources of error in previous PCM calculations[39] are analyzed, and applicability of the dielectric continuum approach for modeling reaction free-energy profiles is established.

II. METHODOLOGY

Let us consider an $A\rightarrow B$ reaction. The standard free energies of reaction in the gas phase and in solution are denoted as ΔG_g^0 and ΔG_s^0, respectively. Associating with the reactant A and product B are free energies of solvation denoted as $\Delta G_{\rm solv}^0$. From the thermodynamic cycle given below

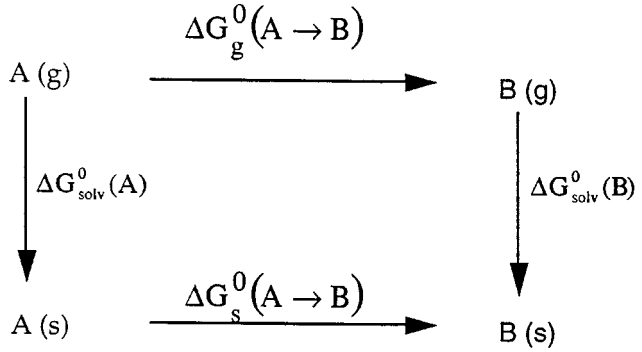

the standard free energy of the reaction in solution can be written as

$$\Delta G_s^0=\Delta G_g^0+[\Delta G_{\rm solv}^0(B)-\Delta G_{\rm solv}^0(A)], \tag{1}$$

where the gas-phase free energy is given by

$$\Delta G_g^0=\Delta E-RT\ \ln\left(\frac{Q^B}{Q^A}\right). \tag{2}$$

Here ΔE is the reaction energy; R is the Boltzmann constant; T is the temperature; Q^A and Q^B are the total partition functions evaluated with the zero of energy set at the bottom of each respective potential well.

We can generalize this expression for the free-energy profile of reaction in solution. In particular, the standard free energy at a point $\mathbf{R}(s)$ along the reaction coordinate s relative to that of the reactant A is expressed as

$$\begin{aligned}\Delta G_s^0(s)&=\Delta G_s^0[A\rightarrow\mathbf{R}(s)]\\&=V_{\rm MEP}(s)-RT\ \ln\left\{\frac{Q[\mathbf{R}(s)]}{Q^A}\right\}\\&\quad+\Delta G_{\rm solv}^0[\mathbf{R}(s)]-\Delta G_{\rm solv}^0(A),\end{aligned} \tag{3}$$

where $V_{\rm MEP}(s)$ is the potential energy along the gas-phase minimum energy path with the zero of energy set at the reactant. Equation (3) indicates that in order to obtain accurate free-energy profile for reaction in solution, one requires to have not only accurate free energy of solvation but also accurate gas-phase free-energy profile. This point has often been overlooked in many previous studies.

The central point needs to be discussed here is the determination of the reaction coordinate s. The simplest approach, adopted in most studies to date, is to define s as the distance along the minimum energy path on the gas-phase potential-energy surface. Then, using the static equilibrium solvation approach the free-energy profile in solution can be estimated by adding free energy of solvation to the gas-phase free-energy profile along this reaction coordinate. As mentioned earlier, this approach can be erroneous if solvation significantly changes the topology of the free-energy surface relative to the gas-phase potential-energy surface. In this case, one should include solvent effects in the determination of the reaction coordinate.

Following the reaction path on the solution-phase free-energy surface, as defined in Eq. (3), is a difficult task. The major difficulty arises from the necessity to perform normal mode analysis at every point on the gas-phase potential surface in order to calculate vibrational partition functions. To circumvent this problem, we first assume that the gas-phase Born–Oppenheimer potential-energy surface $E(\mathbf{R})$ has similar topology to the gas-phase free-energy surface along the reaction coordinate. In this case, we then define a pseudo-free energy surface $G^*(\mathbf{R})$ in the solute nuclear coordinates $\mathbf{R}$ that is related to $E(\mathbf{R})$ by the following expression:

$$G^*(\mathbf{R})=E(\mathbf{R})+\Delta G_{\rm solv}(\mathbf{R}). \tag{4}$$

The pseudo-free energy surface defined above allows one to utilize advanced computational methods that have been well developed for following reaction paths in the gas phase. Analogous to the gas phase, the reaction coordinate s in solution is defined as the distance along the minimum free-energy path (MFEP) which is the steepest descent path from the transition state toward both the reactant(s) and product(s) on the pseudo-free energy surface $G^*(\mathbf{R})$. To obtain free energy profile of reaction in solution we correct the pseudo-free energy profile $\Delta G^*(s)$ for the gas-phase $-RT\ \ln(Q(s)/Q^A)$ term along the solution-phase reaction coordinate. The central approximation here is that in the determination of the solution-phase reaction coordinate the $-RT\ \ln(Q(s)/Q^A)$ term does not have significant contribution thus can be ignored.

Within the dielectric continuum solvation methodology, we can write the free energy of solvation as

$$\begin{aligned}\Delta G_{\rm solv}(\mathbf{R})&=\Delta G_{\rm el}(\mathbf{R})+\Delta G_{\rm dis}(\mathbf{R})+\Delta G_{\rm rep}(\mathbf{R})\\&\quad+\Delta G_{\rm cav}(\mathbf{R}),\end{aligned} \tag{5}$$

where $\Delta G_{\rm el}$ constitutes solvation terms of electrostatic nature; $\Delta G_{\rm dis}$ and $\Delta G_{\rm rep}$ are the solvent–solute dispersion and repulsion interactions, respectively; $\Delta G_{\rm cav}$ is the work required to create the cavity. Note that contributions from the

solute internal motions, such as shifts in the solute vibrational frequencies, are effectively included by fitting the cavity size to experimental free energies of hydration.

For polar solvents such as water, the electrostatic term makes the largest contribution to the solvent effects. For this term, we used the GCOSMO model[30–35] which was generalized from the COSMO approach which was originally implemented at the semiempirical MO level[36] for a more accurate and general description for the solute charge density without using the multipole expansion and for inclusion of nonelectrostatic contributions. The essence of the GCOSMO model is to determine first the surface charges $\sigma(\mathbf{r})$ on the surface (S) of the cavity in a screening conductor (the dielectric constant $\epsilon=\infty$) from a boundary condition that the electrostatic potential on the surface S is zero

$$\sum_i \frac{z_i}{|\mathbf{r}-\mathbf{R}_i|} - \int_V \frac{\rho(\mathbf{r}')}{|\mathbf{r}-\mathbf{r}'|}\, d^3r' + \int_S \frac{\sigma(\mathbf{r}')}{|\mathbf{r}-\mathbf{r}'|}\, d^2r' = 0, \tag{6}$$

where $\mathbf{r}$ is on S; ρ is the solute electron density; and z_i and $\mathbf{R}_i$ are the nuclear charge and position vector of atom i. For a dielectric medium specified by the dielectric constant ϵ, the surface charges are then determined approximately by scaling the screening conductor surface charge σ by a factor of $f(\epsilon)=(\epsilon-1)/\epsilon$ to satisfy Gauss' theorem. This is a good approximation to the exact boundary condition used in the PCM model. Average unsigned differences in hydration free energies between two models are less than 0.2 kcal/mol for neutral solutes and 0.9 kcal/mol for ions.[31]

Within the boundary element approach, the cavity boundary is defined by M surface elements with areas $\{S_u\}$. The surface charge density at each surface element is approximated as a point charge, $\{q_u\}$, located at the center of that element, $\{t_u\}$. From the above boundary condition, the total electrostatic free energy of the whole system (solute+surface charges) is then given by

$$G_{\mathbf{el}} = \sum_{\mu\nu} P_{\mu\nu}(H_{\mu\nu} + \tfrac{1}{2}G_{\mu\nu}) - \tfrac{1}{2} f(\epsilon)\mathbf{z}^{\mathbf{+}}\mathbf{B}^{\mathbf{+}}\mathbf{A}^{\mathbf{-1}}\mathbf{B}\mathbf{z} + E_{nn}, \tag{7}$$

where E_{nn} is the solute nuclear repulsion and $\mathbf{z}$ is the vector of N nuclear charges. The solvent contributions to the one and two electron terms of the Fock matrix ($H_{\mu\nu}$ and $G_{\mu\nu}$, respectively) are expressed as

$$H^s_{\mu\nu} = -f(\epsilon)\mathbf{z}^{\dagger}\mathbf{B}^{\dagger}\mathbf{A}^{-1}\mathbf{L}_{\mu\nu}, \tag{8}$$

$$G^s_{\mu\nu} = -f(\epsilon)\mathbf{c}^{\dagger}\mathbf{A}^{-1}\mathbf{L}_{\mu\nu}. \tag{9}$$

where $\mathbf{A}$, $\mathbf{B}$, and $\mathbf{c}$ are $M\times M$, $M\times N$, and $M\times 1$ matrices, respectively, with matrix elements defined by

$$A_{uv} = \frac{1}{|\mathbf{t}_u - \mathbf{t}_v|} \quad \text{for } u\neq v, \quad \text{and} \quad A_{uu} = 1.07\sqrt{\frac{4\pi}{S_u}}, \tag{10}$$

$$B_{ui} = \frac{1}{|\mathbf{t}_u - \mathbf{R}_i|}, \tag{11}$$

$$c_u = \sum_{\mu\nu} P_{\mu\nu} L^u_{\mu\nu} \tag{12}$$

where

$$L^u_{\mu\nu} = -\left\langle \mu \left| \frac{1}{\mathbf{r}-\mathbf{t}_u} \right| \nu \right\rangle, \tag{13}$$

and $P_{\mu\nu}$ is the density matrix element.

For the dispersion and short-range repulsion contributions, we adopted Floris *et al.* method.[40] For the cavity formation term, we employed the scaled particle fluid theory of Pierotti,[41] which was transformed by Huron and Claverie[42] into an atom–molecule-type formalism. These methods have been found to be sufficiently accurate from several previous studies[30,40,43–48] including our own.

The solvent excluding surface[49] was used for defining the cavity boundary due to its smooth nature. It was constructed using the GEPOL algorithm.[50] The atomic radii (N: 1.74; C: 2.10; H: 1.17; Cl: 1.75 Å) used in this study have been optimized at the HF/6-31G(d) level to reproduce free energies of hydration for a representative set of small molecules and ions.[31] By optimizing the atomic radii for determining the cavity size we effectively account for other contributions that were not explicitly considered in the model. One of such contributions is the outlying charge effect. This effect arises from the fact that implementation of any classical continuum solvation model within a quantum mechanical level will lead to a small portion of the electronic density distribution being outside of the cavity regardless of the cavity size. Recent studies[51,52] have proposed several post-SCF correction schemes accounting for this effect. In our view, such schemes add an order of complication when one requires to include the outlying charge effect in free energy derivatives for consistency as in the determination of reaction path, yet the atomic radii are still needed to be optimized to account for other effects. As pointed in previous studies,[51,52] the outlying charge effect is large for anions such as Cl^- in this study and shows a noticeable basis set dependence. Such effect is an interesting subject for investigation on its own. Since our focus here is on free-energy profile of reaction in solution, we will discuss the outlying charge effect in a forthcoming paper. For this study, however, as seen in Table I, using the 6-31G(d,p) basis set our atomic radii yield free energies of hydration of ions in less than 6% difference with the experimental data. This is within the experimental uncertainty for solvation free energies of ions. Since the outlying charge effect is expected to be somewhat smaller at points along the reaction path than at the ion products, it would not be totally canceled in calculations of free-energy profile. One would expect an error in the free-energy profile of less than 6% in this case.

III. COMPUTATIONAL APPROACH

Calculations of a reaction profile first required optimizations of the reactants, products, and transition state in solution. These were done using analytical first derivatives of the electrostatic free energy [Eq. (7)].[33] For application given

TABLE I. Geometries (distances in Å, angles in degrees), dipole moments μ (Debye), and hydration free energies (kcal/mol) of the reactants, products, and transition state of the $NH_3+CH_3Cl \leftrightarrow H_3NCH_3^+ + Cl^-$ reaction in the gas phase and in aqueous solution

	Gas phase		Aqueous solution	
	BH&HLYP	MP2	BH&HLYP	MP2
		NH_3		
NH	1.004	1.013	1.010	1.015
∠HNH	108.7	106.1	105.4	104.7
μ	1.696	1.924	2.237	2.337
ΔG_{hyd}			−6.5(−4.3)[a]	−6.4
		CH_3Cl		
CCl	1.785	1.776	1.800	1.788
CH	1.081	1.084	1.080	1.082
∠HCCl	108.5	110.0	107.8	108.3
μ	2.129	2.212	2.757	2.865
ΔG_{hyd}			−2.2(−0.6)[a]	−1.7
		$H_3NCH_3^+$		
CN	1.502	1.507	1.484	1.490
NH	1.017	1.023	1.019	1.025
CH	1.081	1.084	1.082	1.084
∠HNC	111.5	111.5	111.5	111.5
∠HCN	108.3	108.1	108.4	108.3
ΔG_{hyd}			−69.8(−68)[a]	−69.9
		Cl^-		
ΔG_{hyd}			−79.3(−75)[a]	−79.0
		$[H_3N\cdots CH_3\cdots Cl]^{\ddagger}$ TS		
CN	1.798[1.66][b]	1.793	2.215[1.96][b]	2.156
CCl	2.484[2.09][b]	2.443	2.183[1.94][b]	2.170
CH	1.070	1.073	1.069	1.073
NH	1.010	1.017	1.009	1.015
∠HNC	110.5	110.8	111.5	111.7
∠HCN	99.4	98.8	85.6	85.9

[a]Values in parentheses are experimental hydration energies taken from Ref. 29.
[b]Values in square brackets are for AM1 transition state geometry in the gas phase and in aqueous solution. Taken from Ref. 20.

below, the electrostatic term is dominant, thus neglecting derivative contributions from the nonelectrostatic terms is expected to yield negligible errors. As discussed below, our present results confirm this expectation.

The minimum energy path (MEP) on the gas-phase potential-energy surface and the minimum free-energy path (MFEP) on the liquid-phase pseudo-free energy surface were determined by using the second-order reaction path following method developed by Schlegel and co-workers.[53] Step-size of 0.1 amu$^{1/2}$ bohr was used. Reaction path calculations require the normal mode analysis at the transition state. For the reaction in solution, such analysis has been done by numerical differentiation of the free-energy gradient. Implementation of the analytical second free-energy derivatives for the equilibrium GCOSMO solvation approximation is in progress. To calculate the temperature dependent $-RT\ \ln(Q(s)/Q^A)$ term we performed gas-phase Hessian calculations for a small number of points along the solution-phase reaction coordinate.

The choice of the basis set and calculation method is discussed in detail in the next section. All calculations were done using our locally modified GAUSSIAN92/DFT program.[54] It is important to note that GCOSMO calculations in solution are only 10%–20% more time consuming than gas-phase molecular calculations.

IV. RESULTS AND DISCUSSION

A. Accuracy comparison between BH&HLYP and MP2 methods

In our previous studies[30,31,34] for a large set of molecules and ions, we found that free energies of solvation obtained from HF, MP2, and DFT methods are very similar. Therefore, the choice of the adequate method should be based on their ability to accurately represent the gas-phase potential-energy surface. Nonlocal DFT methods are particularly attractive since they are computational less demanding than even MP2, especially for large systems.

Investigations on the accuracy of DFT methods have been an active area of research. The B3LYP method has been the most popular choice for many applications due to its good performance for equilibrium properties.[55] Reaction rate constants, however, are rather sensitive to the transition state region and the shape of the potential-energy surface along the MEP. Therefore, inspection of these properties is also important for the choice of appropriate method. From

TABLE II. Reaction energies and barrier heights (kcal/mol) of the Menshutkin $NH_3+CH_3Cl \leftrightarrow H_3NCH_3^+ + Cl^-$ reaction in the gas phase and in aqueous solution.

	MP2	MP4(SDTQ)	BH&HLYP	Expt.
		Gas phase		
ΔE	121.0	114.0	116.5	
ΔG	128.3	121.3	124.0	110[a]
$\Delta V^{\ddagger}$	38.4	32.1	32.6	
$\Delta G^{\ddagger}$	51.4	45.1	45.7	
		Aqueous solution		
ΔG	−19.8		−16.5	-34 ± 10[b]
$\Delta G^{\ddagger}$	31.4		24.8	23.5[c]

[a]Taken from Ref. 20.
[b]Estimated from experimental free energies of hydration and standard free energy of formation (see also Ref. 20).
[c]Experimental data for the $NH_3+CH_3I \leftrightarrow H_3CNH_3^+ + I^-$ reaction in water (Ref. 65).

several our studies on the accuracy of DFT methods for reaction profiles (including $S_N2Cl^- + CH_3Cl$ reaction[32]) and reaction rates,[56–59] we found that among existing DFT methods, the combination of the hybrid Becke's half-and-half for exchange and Lee–Yang–Parr for correlation (BH&HLYP)[60,61] gives the best overall performance.

In this study, we compare the accuracy of the MP2[62] and BH&HLYP methods using the 6-31G(d,p) basis set. First, we optimized geometries of the reactants, products and transition state in C_{3v} symmetry in the gas phase and in aqueous solution using both methods. Note that on the gas-phase potential-energy surface, there exists a stable complex $H_3NCH_3\cdots Cl$ in the product channel. We found that at the BH&HLYP/6-31G(d,p) level, the linearlike complex (C_{3v} symmetry) has negligible stabilization energy relative to the transition state. Gordon and Webb[63] pointed out that due to a zwitterionic character, the bendlike complex (the angle NCCl is less than 180°) is much more stable. In water, the zwitterion, if exists, would prefer to have a linearlike structure due to larger solvation free energy.[31] However, we found that no such stable complex exists in aqueous solution and thus no further attention is given for determination of the most stable complex on the gas-phase potential surface.

Geometrical parameters, dipole moments, and hydration free energies of the reactants, products, and transition state are listed in Table I. As expected, hydration free energies calculated from both methods are very similar with the largest difference of only 0.5 kcal/mol. To investigate the accuracy of these methods for the gas-phase potential surface, we performed benchmark single point MP4(SDTQ) calculations at the MP2 optimized geometries using a larger aug-cc-pVDZ[64] basis set. This is the most accurate calculation of this system to date. Reaction and activation free energies computed by all three methods are compared with available experimental data in Table II. As compared to MP4 calculations, MP2 overestimates the classical reaction barrier ($\Delta V^{\ddagger}$) by 6.3 kcal/mol while BH&HLYP agrees to within 0.5 kcal/mol. Although all three methods yield too large reaction free energies ΔG (the same order of magnitude for this error was also observed in Gao and Xia's MP4 calculations[20] using a smaller basis set), the BH&HLYP result is closer to both MP4 and experiment than the MP2 result. In addition, an excellent agreement was found between MP4 and BH&HLYP calculated free energies of activation $\Delta G^{\ddagger}$.

In agreement with our previous finding, we conclude that the BH&HLYP method is computationally cheaper and yields more accurate results than MP2. Consequently, it is the method of choice for further calculations and the remaining discussion will be based on the BH&HLYP results.

B. Solvent effects on geometry and electronic structure

Aqueous solvent has noticeable effects on the equilibrium geometries of the polar reactants molecules and product ions as shown in Table I. For NH_3, solvent water molecules compress the HNH angle from 108.7° to 105.4° and elongate the NH bond from 1.004 to 1.010 Å. Similar effects are seen for CH_3Cl, where the CCl bond is elongated by 0.015 Å and the HCCl angle is compressed by less than 0.7°. However, it is different for $H_3CNH_3^+$ ion, where the CN bond is shortened by 0.018 Å upon solvation. These results indicate that in addition to the solvent polarization, the solute polarization, i.e., the feedback of the solute to the solvent polarization field, is also important.

In Fig. 1 we plotted the CN and CCl bond distances and the HCN angle along both the gas-phase MEP and solution-phase MFEP. These internal coordinates show the largest changes as functions of the reaction coordinate. For reaction in water, they are shifted in the product direction. This means solvent effects advance the reaction coordinate. In particular, at the transition state solvent effect elongates the CN bond by 0.42 Å, shortens the CCl bond by 0.30 Å and reduces the HCN angle by 14°. These trends are consistent with previous results from PCM model[39] and semiempirical AM1/MM simulations.[20] This can be understood from the fact that the Menshutkin reaction is a charge separation process. Aqueous solvent facilitates charge transfer and increases the dipole moment by gaining favorable free energy of solvation. This is also seen from Figs. 2 and 3 where we plot the dipole moment of the solute and the Mulliken charge of the Cl atom along the reaction coordinate.

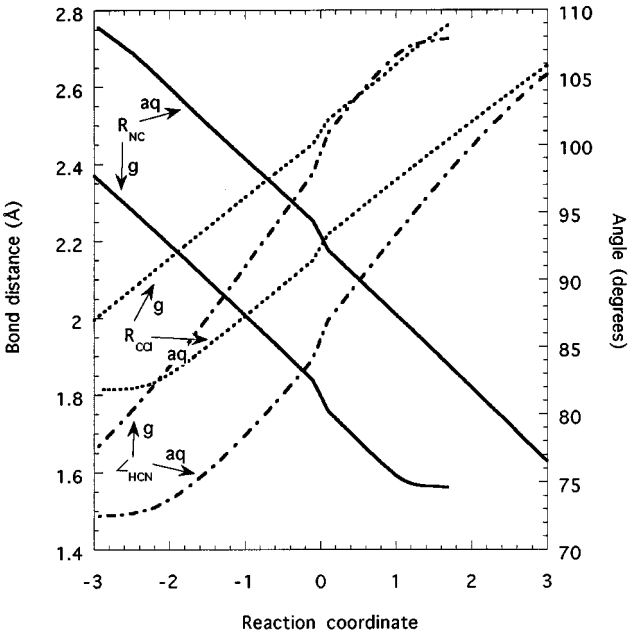

FIG. 1. Bond distances NC and CCl and angle HCN as functions of the reaction coordinates for the Menshutkin NH_3+CH_3Cl reaction in both the gas phase (g) and aqueous solution (aq). Origin of the reaction coordinate is at the saddle point in each case.

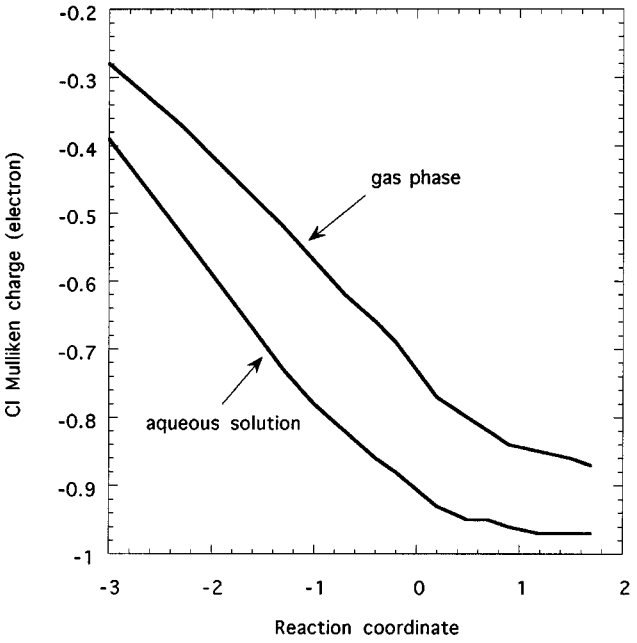

FIG. 3. Plot of the Mulliken charge on the Cl atom as function of the reaction coordinate.

C. Solvent effects on reaction profile

Heats of reaction and activation free energies are listed in Table II. Free-energy profiles in both the gas phase and aqueous solution are also plotted in Fig. 4. As mentioned earlier, our BH&HLYP calculations overestimate the gas-phase free energy of reaction by 14 kcal/mol. As consequence, our calculated free energy of reaction in water (-16.5 kcal/mol) is in good agreement with the AM1/MM result of -18 kcal/mol, but both are too high compared to the experimental estimate of -34 ± 10 kcal/mol.[20] If experimental gas-phase free energy of reaction were used, both GCOSMO and AM1/MM free energies of reaction in water would fall within the experimental uncertainty.

Our calculated gas-phase free energy of activation at the room temperature (45.7 kcal/mol) is consistent with Gao and

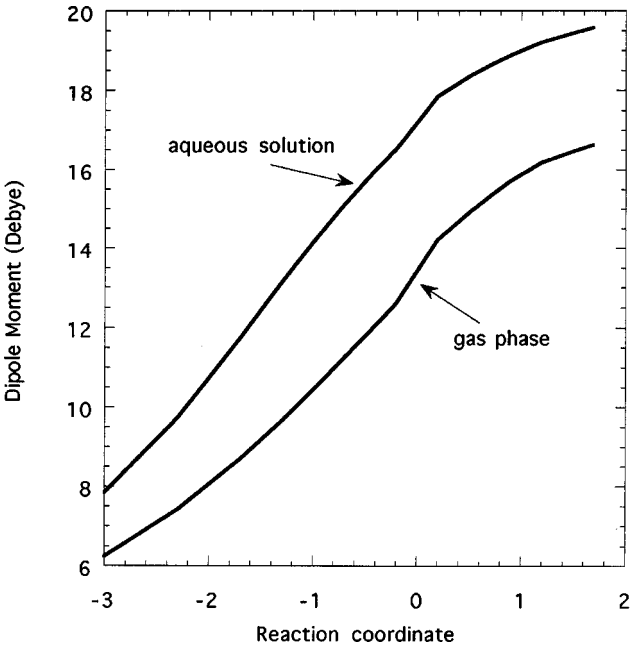

FIG. 2. Plot of the dipole moment of the reacting system as function of the reaction coordinate.

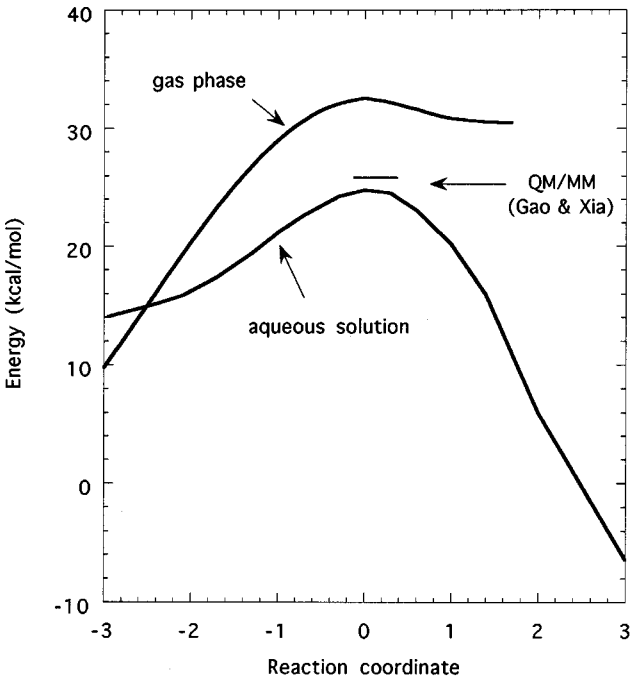

FIG. 4. Potential energy profile along the gas phase MEP and free-energy profile along the solution-phase MFEP. QM/MM free energy of activation is taken from Ref. 20.

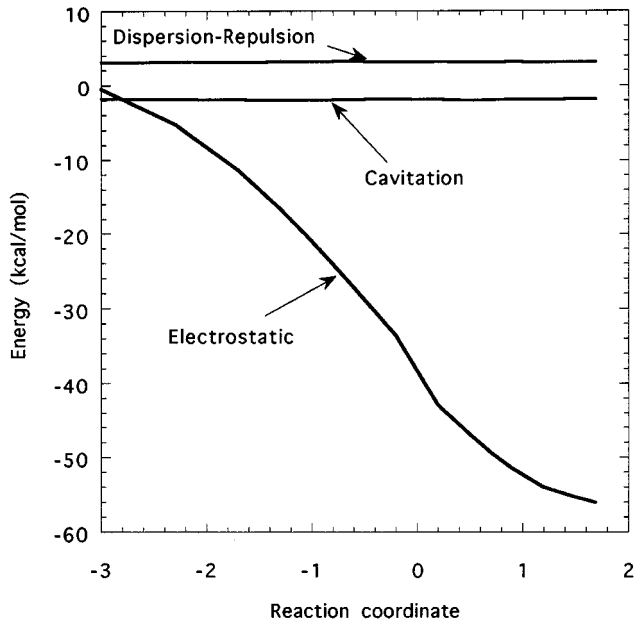

FIG. 5. Individual contributions, i.e., electrostatic, dispersion–repulsion, and cavitation, to the free energy of hydration along the reaction coordinate.

Xia's best estimate of 46.7 kcal/mol. This activation energy is only relevant to the formation of the gas-phase $H_3NCH_3\cdots Cl$ complex from the reactants. For formation of ion products $H_3CNH_3^+$ and Cl^-, the reaction is 110 kcal/mol endothermic. Thus, the dynamical bottleneck is located far in the exit channel. Solvent effect changes the reaction energetics to noticeably exothermic thus shifts this bottleneck significantly to the entrance channel and decreases the free energy of activation to 24.8 kcal/mol. This free energy of activation agrees well with Gao and Xia's AM1/MM simulations (26.3 kcal/mol) and experimental value for a similar Menshutkin reaction NH_3+CH_3I in water (23.5 kcal/mol in Ref. 65). The agreement between GCOSMO results and AM1/MM simulations leads to an important conclusion that electrostatic solvent–solute interaction not specific hydrogen bond interaction as infered by Gao and Xia makes the major contribution to the transition state stabilization in the type II SN_2 reactions. This conclusion is further supported by examining individual contributions to the solvation free energy along the reaction coordinate as shown in Fig. 5. Furthermore, the relatively small contributions of the dispersion–repulsion and cavitation to the free energy of hydration compared to the electrostatic term support the use of only electrostatic free energy derivative in our structure determinations as mentioned earlier. In conclusion, simple (even without explicit water molecules) dielectric continuum models should be applicable for studying these reactions.

Previous dielectric continuum calculations done by Sola *et al.* for the NH_3+CH_3Br reaction in water yielded the activation energy of 8.3 kcal/mol. This value appears to be too low. In our opinion, this large error does not necessarily reflect the inaccuracy of the dielectric continuum approach nor indicate the importance of specific solvent–solute interactions but is rather due to several other facts. First, contributions from the solute motions [the $-RT\ \ln(Q^{\ddagger}/Q^{A})$ term in Eq. (3)] was not included. From our present study for the NH_3+CH_3Cl reaction, this term increases the free energy of activation by 13.1 kcal/mol. Second, the calculated gas-phase barrier (21.5 kcal/mol) is probably too low due to neglect of the electron correlation and use of the small 3-21 $+G(d)$ basis set. Finally, these authors did not discuss their selection of atomic radii for cavity construction. Improper radii may significantly contribute to the total error.

V. CONCLUSION

We have presented a general methodology for calculating free energy of activation and reaction profile in solution using the dielectric continuum solvation approach. The availability of efficient free energy derivatives of the GCOSMO model makes it an attractive tool for studying solvent effects on transition state structures, modeling reaction mechanisms in solution and addressing dynamical solvent effects on the reaction coordinate. Using this model, we have carried out a detailed study of the Menshutkin $NH_3+CH_3Cl \rightarrow H_3CNH_3^+ + Cl^-$ reaction in aqueous solution. An excellent agreement between our results and previous elaborous QM/MM simulations confirms the accuracy of the GCOSMO model and its usefulness. In particular, for the Menshutkin reaction, we found that aqueous solvent stabilizes charged products which are unstable in the gas phase. As result, the reaction becomes exothermic in aqueous solution and has the free energy of activation at the room temperature of about 24.8 kcal/mol. This result is consistent with available experimental data on a similar NH_3+CH_3I reaction in water. In addition, aqueous solvent shifts the transition state significantly to the reactant channel and advances the reaction coordinate. Nonequilibrium dynamical solvent effects are expected to have smaller contribution to the reaction rate for this reaction. It is however a fundamentally important aspect of reaction in solution and will be addressed in a future study. Reaction path determination discussed in this paper is a first important step in this direction.

ACKNOWLEDGMENT

This work is supported in part by the National Science Foundation via a Young Investigator Award to T.N.T.

[1] *Structure and Reactivity in Aqueous Solution: Characterization of Chemical and Biological Systems*, Vol. 568, edited by C. J. Cramer and D. G. Truhlar (American Chemical Society, Washington, D.C., 1994).
[2] A. Warshel, *Computer Modeling of Chemical Reactions in Enzymes and Solutions* (Wiley, New York, 1991).
[3] J. Tomasi, B. Mennucci, R. Cammi, and M. Cossi, in *Theoretical Aspects of Biochemical Reactivity*, edited by G. Náray-Szabó and A. Warshel (1996), to be published.
[4] R. Car and M. Parrinello, Phys. Rev. Lett. **55**, 2471 (1985).
[5] K. Laasonen, M. Sprik, M. Parrinello, and R. Car, J. Chem. Phys. **99**, 9080 (1993).
[6] E. S. Fois, M. Sprik, and M. Parrinello, Chem. Phys. Lett. **223**, 411 (1994).
[7] A. Pullman and B. Pullman, Q. Rev. Biophys. **7**, 505 (1975).
[8] K. Morokuma, J. Am. Chem. Soc. **104**, 3732 (1982).
[9] W. L. Jorgensen, Acc. Chem. Res. **22**, 184 (1989).
[10] J. Aqvist and A. Warshel, Chem. Rev. **93**, 2523 (1993).

[11] J. Gao, in *Reviews in Computational Chemistry*, edited by K. B. Lipkowitz and D. B. Boyd (VCH, New York, 1996), Vol. 7, p. 119.
[12] U. C. Singh and P. A. Kollman, J. Comput. Chem. **7**, 718 (1986).
[13] M. J. Field, in *Computer Simulation of Biomolecular Systems: Theoretical and Experimental Applications* Vol. 2, edited by W. F. van Gunsteren, P. K. Weiner, and A. J. Wilkinson (ESCOM, Leiden, 1993), p. 82.
[14] J. J. Field, P. A. Bash, and M. Karplus, J. Comp. Chem. **11**, 700 (1990).
[15] P. N. Day, J. H. Jensen, M. S. Gordon, S. P. Webb, W. J. Stevens, M. Krauss, D. Garmer, H. Basch, and D. Cohen, J. Chem. Phys. **105**, 1968 (1996).
[16] C. Cativiela, J. I. García, J. A. Mayoral, A. Royo, J., L. Salvatella, X. Assfeld, and M. F. Ruiz-López, J. Phys. Org. Chem. **5**, 230 (1992).
[17] M. F. Ruiz-López, X. Assfeld, J. I. García, J. A. Mayoral, and L. Salvatella, J. Am. Chem. Soc. **15**, 8780 (1993).
[18] X. Assfeld, M. F. Ruiz-López, J. I. García, Mayoral, J. A., and L. Salvatella, J. Chem. Soc., Commun. 1371 (1995).
[19] X. Assfeld, J. A. Sordo, J. Gonzalez, M. F. Ruizlopez, and T. L. Sordo, J. Mol. Struct. (Theochem) **106**, 193 (1993).
[20] J. Gao and X. Xia, J. Am. Chem. Soc. **115**, 9667 (1993).
[21] C. J. Cramer and D. G. Truhlar, in *Reviews in Computational Chemistry*, Vol. 6, edited by K. B. Lipkowitz and D. B. Boyd (VCH, New York, 1994), p. 1.
[22] C. J. Cramer and D. G. Truhlar, in *Solvent Effects and Chemical Reactivity*, edited by O. Tapia and J. Bertrán (Kluwer, Dordrecht, 1996).
[23] J. Tomasi and M. Persico, Chem. Rev. **94**, 2027 (1994).
[24] S. Miertuš, E. Scrocco, and J. Tomasi, Chem. Phys. **55**, 117 (1981).
[25] R. Cammi and J. Tomasi, J. Chem. Phys. **100**, 7495 (1994).
[26] R. Cammi and J. Tomasi, J. Chem. Phys. **101**, 3888 (1994).
[27] M. Cossi, J. Tomasi, and R. Cammi, Int. J. Quantum Chem. **S29**, 695 (1995).
[28] V. Dillet, D. Rinaldi, J. G. Angyan, and J. L. Rivail, Chem. Phys. Lett. **202**, 18 (1993).
[29] V. Dillet, D. Rinaldi, and J. L. Rivail, J. Phys. Chem. **98**, 5034 (1994).
[30] T. N. Truong and E. V. Stefanovich, Chem. Phys. Lett. **240**, 253 (1995).
[31] E. V. Stefanovich and T. N. Truong, Chem. Phys. Lett. **244**, 65 (1995).
[32] T. N. Truong and E. V. Stefanovich, J. Phys. Chem. **99**, 14700 (1995).
[33] T. N. Truong and E. V. Stefanovich, J. Chem. Phys. **103**, 3709 (1995).
[34] T. N. Truong, U. N. Nguyen, and E. V. Stefanovich, Int. J. Quantum Chem. **60**, 1615 (1996).
[35] E. V. Stefanovich and T. N. Truong, J. Chem. Phys. **105**, 2961 (1996).
[36] A. Klamt and G. Schüürmann, J. Chem. Soc., Perkin Trans. II, 799 (1993).
[37] J. Andzelm, C. Kölmel, and A. Klamt, J. Chem. Phys. **103**, 9312 (1995).
[38] N. S. Issacs, *Physical Organic Chemistry* (Wiley, New York, 1987).
[39] M. Solà, A. Lledós, M. Duran, J. Bertrán, and J.-L. M. Abboud, J. Am. Chem. Soc. **113**, 2873 (1991).
[40] F. M. Floris, J. Tomasi, and J. L. P. Ahuir, J. Comp. Chem. **12**, 784 (1991).
[41] R. A. Pierotti, Chem. Rev. **76**, 717 (1976).
[42] M. J. Huron and P. Claverie, J. Phys. Chem. **76**, 2123 (1972).
[43] M. A. Aguilar and F. J. Olivares del Valle, Chem. Phys. **138**, 327 (1989).
[44] F. Floris and J. Tomasi, J. Comp. Chem. **10**, 616 (1989).
[45] F. M. Floris, A. Tani, and J. Tomasi, Chem. Phys. **169**, 11 (1993).
[46] V. Frecer, S. Miertuš, and M. Majekova, J. Mol. Struct. (Theochem) **73**, 157 (1991).
[47] F. J. Olivares del Valle and M. A. Aguilar, J. Mol. Struct. (Theochem) **99**, 25 (1993).
[48] D. Rinaldi, B. J. C. Cabral, and J. L. Rivail, Chem. Phys. Lett. **125**, 495 (1986).
[49] F. M. Richards, Ann. Rev. Biophys. Bioeng. **6**, 151 (1977).
[50] J. L. Pascual-Ahuir, E. Silla, and I. Tuñon, J. Comp. Chem. **15**, 1127 (1994).
[51] R. Cammi and J. Tomasi, J. Comput. Chem. **16**, 1449 (1995).
[52] A. Klamt and V. Jonas, J. Chem. Phys. **105**, 9972 (1996).
[53] C. Gonzalez and H. B. Schlegel, J. Phys. Chem. **94**, 5523 (1990).
[54] GAUSSIAN92, M. J. Frisch, G. W. Trucks, H. B. Schlegel, P. M. W. Gill, B. G. Johnson, M. W. Wong, J. B. Foresman, M. A. Robb, M. Head-Gordon, E. S. Replogle, R. Gomperts, J. L. Andres, K. Raghavachari, J. S. Binkley, C. Gonzalez, R. L. Martin, D. J. Fox, D. J. Defrees, J. Baker, J. J. P. Stewart, and J. A. Pople, G92/DFT, Revision G.3 (Gaussian, Inc., Pittsburgh, 1993).
[55] B. G. Johnson, P. M. W. Gill, and J. A. Pople, J. Chem. Phys. **98**, 5612 (1993).
[56] R. Bell and T. N. Truong, J. Chem. Phys. **101**, 10442 (1994).
[57] W. T. Duncan and T. N. Truong, J. Chem. Phys. **103**, 9642 (1995).
[58] T. N. Truong and W. T. Duncan, J. Chem. Phys. **101**, 7408 (1994).
[59] T. N. Truong, W. T. Duncan, and R. L. Bell, in *Chemical Applications of Density Functional Theory*, Vol. 629, edited by B. B. Laird, R. B. Ross, and T. Ziegler (American Chemical Society, Washington, D.C., 1996), p. 85.
[60] A. D. Becke, J. Chem. Phys. **98**, 1372 (1993).
[61] C. Lee, W. Yang, and R. G. Parr, Phys. Rev. B **37**, 785 (1988).
[62] C. Möller and M. S. Plesset, Phys. Rev. **46**, 618 (1934).
[63] M. S. Gordon and S. Webb (private communication).
[64] D. E. Woon and T. H. Dunning, Jr., J. Phys. Chem. **98**, 1358 (1993).
[65] K. Okamoto, S. Fukui, and H. Shingu, Bull. Chem. Soc. Jpn. **40**, 1920 (1967).